Spin stabilized magnetic levitation

Martin D. Simon[a)]
Department of Physics, University of California at Los Angeles, 405 Hilgard Avenue, Los Angeles, California

Lee O. Heflinger
5001 Paseo de Pablo, Torrance, California 90505-6228

S. L. Ridgway
537 9th St., Santa Monica, California 90402

(Received 30 August 1996; accepted 28 January 1997)

The stability of the Levitron® cannot be explained if the top's axis has a fixed direction in space. Stability against flipping is not enough. Gyroscopic precession around the local magnetic field direction is necessary. An analysis and numerical integration of the equations of motion for an experimental stemless top that includes gyroscopic precession around the local magnetic field lines predict that the top will be supported stably up to spin speeds of about 3065 rpm. An upper spin limit of 2779 rpm for this top is observed experimentally and explained as an adiabatic condition. Spin stabilized magnetic levitation is a macroscopic analog of magnetic gradient traps used to confine particles with a quantum magnetic moment.

I. INTRODUCTION

The Levitron®[1] (Ref. 1) is a remarkable toy which levitates in air a 22-g spinning permanent magnet in the form of a small handspun top. The top is spun on a lifter plate on a permanent magnet base and then raised to the levitation height. The top floats about 3.2 cm above the base for over 2 min until its spin rate declines due to air resistance to about 1000 rpm. Unlike an earlier magnet toy which requires a thrust bearing plate to stabilize motion along one direction,[2] the magnetic top floats freely above the base magnet and is fully trapped in three dimensions (see Fig. 1). Since Earnshaw's theorem of 1842[3] rules out stable magnetic levitation for static magnetic dipoles, it was not obvious to us how the Levitron worked. A simple theory of gyroscopic stability against flipping proposed by the manufacturer and others[4,5] is not sufficient to explain the stability.

Magnetic levitation of spinning permanent magnet tops was discovered by inventor Roy Harrigan who patented it in

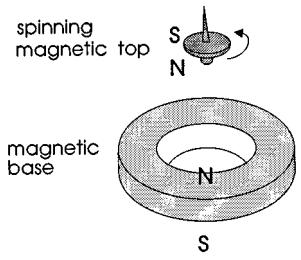

Fig. 1. General configuration for spin stabilized magnetic levitation. The commercial Levitron actually has a solid square base uniformly magnetized except for a circular region in the center. Ring magnets work fine despite some patent claims that it is impossible to levitate over circular magnets (Ref. 4).

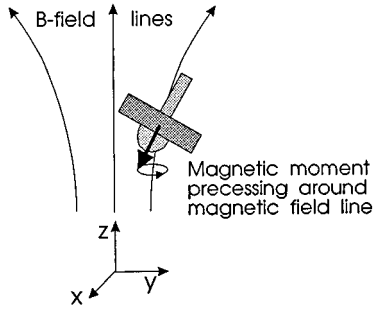

Fig. 2. As the top moves off center, its precession axis orients to the local field direction. Without this reorientation, radial confinement would be impossible at the levitation height.

1983.[6] Harrigan persisted in his efforts even after being told by several physicists that permanent magnet levitation was impossible and that he was wasting his time.[7] Besides discovering spin stabilization Harrigan designed a square dish-shaped base that established a suitable magnetic field configuration, made a top with the right rotational inertia, mass, and magnetic moment, found the small capture volume, and invented a means of moving the spinning top to the right location. The parameter space for successful levitation is quite small.

Not much happened with the invention until 1993 when Bill Hones of Fascinations learned of Harrigan's patent and saw a working prototype of the levitating top. Hones and Harrigan had a brief collaboration to make and market a levitating top toy but it soon ended.[7,8] In 1994 Bill Hones and his father applied for a patent on a levitating top that used a square permanent magnet base, which was issued in 1995.[4] The Levitron, made by Fascinations, has a square base magnet with a region of weaker or null magnetization in the center. The Hones' patent states that levitation over a circular base magnet is not possible. We routinely use circular ring magnets which work at least as well as a square base.

Our investigation included measurements of the commercial toy as well as modified experimental versions. We used air jets and then electromagnetic drives to counter the effects of air resistance and to spin the top faster. We also numerically integrated the equations of motion to determine the stability limits and compare to our calculations and experiments. Our most interesting finding is that there is a maximum spin limit beyond which the top is unstable and cannot be confined. Understanding this feature is essential to understanding the actual trapping mechanism.

While writing this paper, we became aware of a paper by Dr. Michael Berry, now published in the Proceedings of the Royal Society of London.[9] He was kind enough to send us a preprint of his paper which we highly recommend. Our conclusions about the trapping mechanism are essentially the same as his. Berry develops the theory of the adiabatic invariant further than we do here. We would also like to thank Dr. Berry for reviewing an earlier draft of this paper and making helpful suggestions.

II. HOW IT WORKS

First, it is instructive to see how this trap for magnetic dipoles doesn't work. It is not enough to simply stabilize the top/dipole against flipping. We can consider this the infinite spin case, whether the stability against flipping is provided by spin or by some mechanical arrangement. Assume the top's magnetic dipole moment $\boldsymbol{\mu}$ is always oriented in the vertically downward $-z$ direction and the repulsive magnetic field $\mathbf{B}$ from the base magnet is primarily in the vertically upward $+z$ direction in the levitation region. The potential energy U is $U=-\boldsymbol{\mu}\cdot\mathbf{B}+mgz=\mu B_z+mgz$. There are two conditions for stable levitation. The lifting force $-\mu(\partial B_z/\partial z)$ must balance the weight of the top mg and the potential energy at the levitation point must be a minimum. If the energy is a minimum it must have positive curvature in every direction or $\mu(\partial^2 B_z/\partial x_i^2)>0$, where the x_i are x, y, and z. However, $\nabla^2 B_z=0$ at any point in free space so the energy minimum condition cannot be satisfied in all directions. Instead of a minimum there is a saddle point. This is just a consequence of the fact that the magnetic field in the trapping region is divergence and curl free.

For completeness we note a second way that the trap does not work. We considered that the trap might work by strong focusing. If the top and/or base had nonuniform magnetization, the spinning might create the appropriate time-dependent force to be a stable solution of the Mathieu equation. Measurements of the nonuniformities, the top's inclination, and rotation showed that any focusing forces were too small by many orders of magnitude. Replacing the commercial square-magnetized base with a cylindrically symmetric ring magnet does not degrade the confinement at all, contrary to what one would expect if strong focusing was the trapping mechanism.

The gyroscopic action must do more than prevent the top from flipping. It must act to continuously align the top's precession axis to the local magnetic field direction (see Fig. 2). Under suitable conditions, the component of the magnetic moment along the local magnetic field direction is an adiabatic invariant. When these conditions are met, the potential energy depends only on the magnitude of the magnetic field and gravity. While each component of the magnetic field must satisfy Laplace's equation (i.e., $\nabla^2 B_z=0$), the magnitude of the magnetic field does not. This allows the curvature of the potential energy to be concave up (and not a saddle point) at the levitation height.

Properly understood, the trap mechanism is similar to magnetic gradient traps for neutral particles with a quantum magnetic dipole moment. Such traps were first proposed and used for trapping cold neutrons[10] and are currently used to trap atoms,[11] including recent demonstrations of Bose–Einstein condensation. The spin magnetic moment of a particle such as a neutron along the magnetic field direction is

an adiabatic invariant. If the field does not change too rapidly or go through zero allowing a spin flip, the spin magnetic moment along the magnetic field direction is constant. The potential energy then depends only on the magnitude of the magnetic field. Since localized magnetic field minima are allowed (isolated maxima are prohibited) by the laws of magnetostatics, a trap for antialigned dipoles is possible. Spin polarized particles or atoms seek the weak-field position in magnetic gradient traps.

Another example of a similar adiabatic invariant is the magnetic moment of a charged particle spiraling along a magnetic field line. Here again, if the field changes slowly, the magnetic moment due to the particle orbit perpendicular to the field is constant. A charged particle can be trapped in the low field part of a magnetic mirror.

We make two simplifying assumptions. First we assume that the top is a magnetic dipole whose center is also the center of mass. The position of the center of mass and the dipole are located at the same coordinates **r**. Second, we assume the ''fast'' top condition that the angular momentum is along the spin axis of the top which also coincides with the magnetic moment axis. (We relax the fast top condition in the computer simulation code described in Appendix B.) That is, the angular momentum $\mathbf{L}=I\omega(\boldsymbol{\mu}/\mu)$. Here, I is the rotational inertia of the top around the spin axis, ω is the constant angular spin frequency, and $\boldsymbol{\mu}$ is the magnetic moment. $\mu=|\boldsymbol{\mu}|$ and is constant. The spin ω can have a plus or a minus sign due to the two possible spin directions, parallel or antiparallel to $\boldsymbol{\mu}$, respectively. The sense of the angular momentum does not affect the stability of the top, only the sense of the precession.

The torque and force equations that describe the motion of the top (ignoring air resistance and other losses) are

$$\frac{d\boldsymbol{\mu}}{dt}=\frac{\mu}{I\omega}\,\boldsymbol{\mu}\times\mathbf{B} \tag{1}$$

and

$$m\,\frac{d^2\mathbf{r}}{dt^2}=\boldsymbol{\nabla}(\boldsymbol{\mu}\cdot\mathbf{B})-mg\hat{\mathbf{z}}. \tag{2}$$

The magnetic field is a function of position $\mathbf{B}(\mathbf{r})$ and the magnetic moment depends on both position and time $\boldsymbol{\mu}(\mathbf{r},t)$.

Equation (1) says that the top's spin axis rotates about the direction of the local magnetic field **B** with an angular precession frequency

$$\boldsymbol{\omega}_p=-\frac{\mu\mathbf{B}}{I\omega}\,. \tag{3}$$

It is important to note that the precession frequency is inversely proportional to the spin frequency. Although we have assumed that the top is ''fast,'' if it is too fast, the precession frequency will be too slow to keep the top oriented to the local magnetic field direction. This is the origin of the upper spin limit.

Equation (1) also says that to lowest order, the component of the magnetic moment along the local magnetic field direction is a constant which we can call $\boldsymbol{\mu}_\parallel$. We consider the case shown in Figs. 1 and 2 where $\boldsymbol{\mu}_\parallel$ is antiparallel (repulsive orientation) to **B**. The potential energy of the top is

$$U=-\boldsymbol{\mu}\cdot\mathbf{B}+mgz=|\boldsymbol{\mu}_\parallel|\,|\mathbf{B}|+mgz\approx\mu B+mgz. \tag{4}$$

We can expand the magnetic field around the levitation point as a power series for our cylindrically symmetric geometry

$$B_z=B_0+Sz+Kz^2-\tfrac{1}{2}Kr^2+\cdots, \tag{5}$$

$$B_r=-\tfrac{1}{2}Sr-Krz+\cdots, \tag{6}$$

where

$$S=\frac{\partial B_z}{\partial z}\,,\quad K=\frac{1}{2}\,\frac{\partial^2 B_z}{\partial z^2} \tag{7}$$

and S and K are evaluated at the levitation point. This expansion uses the curl and divergence equations, $\boldsymbol{\nabla}\times\mathbf{B}=0$ and $\boldsymbol{\nabla}\cdot\mathbf{B}=0$, to write the field components in terms of B_z and its derivatives with respect to z. The potential energy becomes

$$U\approx\mu\left[B_0+\left\{\frac{mg}{\mu}+S\right\}z+Kz^2+\frac{1}{2}\,K\,\left\{\frac{(S/2)^2}{B_0K}-1\right\}\,r^2+\cdots\right]. \tag{8}$$

At the levitation point, the expression in the first curly braces must go to zero. The magnetic field gradient balances the force of gravity

$$S=-\frac{mg}{\mu} \tag{9}$$

if the ratio of the mass to the magnetic moment m/μ is correct. This ratio is adjusted by adding small weights to the top. For the potential energy to be a minimum at the trapping point, both K and $\{[(S/2)^2/B_0K]-1\}$ must be positive. The energy well is then quadratic in both r and z and approximates a harmonic oscillator potential. Thus, the trapping condition at the levitation point is

$$\frac{(S/2)^2}{B_0K}-1>0. \tag{10}$$

If the magnetic moment was not free to orient to the local field direction as it moved off center (see Fig. 2), the term in the second curly braces would be only $\{-1\}$, and the top would be unstable radially (for $K>0$). The positive term in the second curly braces represents the energy required to reorient the top's axis from vertical to the local field direction. This reorientation energy creates the radial potential well at the levitation height when the trapping condition in Eq. (10) is satisfied.

Figure 3 shows B, $-S$, K and $[(S/2)^2/B_0K]-1$ for the field of an ideal ring magnet of inner diameter 6 cm and outer diameter 10 cm and shows the trapping region. The trapping height and the stable region have been confirmed by experimental measurements and computer simulation of the equations of motion. The trapping height is above the maximum in the field and just above the inflection point of B_z where the curvature K turns positive. A correctly weighted but non-precessing magnet would be stable in z but unstable in r at this point. Slightly below the levitation point, the top will fall but it is stable in r, which makes it possible to spin the top on the base and raise it into position.

Figure 4 shows an experimental setup for measuring the upper spin limit. A white mark on the spinning top is sensed by the phototransistor and triggers pulses in a drive coil circuit. The phase of the drive is adjusted by rotating the drive coils around the base magnet. The synchronous electromag-

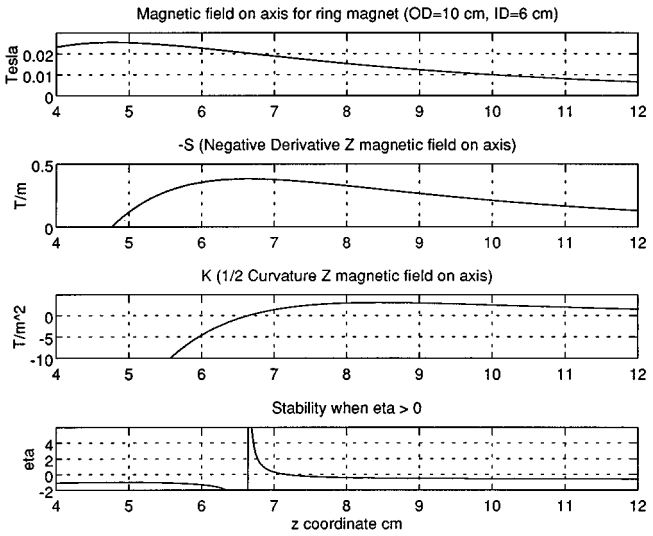

Fig. 3. Graphs of B_z, $-S$, K, and $\eta=[(S/2)^2/B_0K]-1$ as a function of height above an ideal ring magnet with o.d. of 10 cm and i.d. of 6 cm. The stable levitation height occurs where $-S=mg/\mu$, $K>0$, and $[(S/2)^2/B_0K]-1>0$. The levitation height is just above the inflection point of B_z.

netic drive can maintain the top spinning at a constant rate (countering air resistance) or, with increased amplitude, spin it faster. When the top exceeds the maximum stable spin rate it spirals out radially. Appendix A shows one way to calculate the upper spin frequency limit. The system is described by a set of linearized equations which are then solved. The reason for the upper spin limit is that the precession becomes too slow to allow the top to reorient to the local field direction as the top makes its radial excursion in the potential well. The adiabatic condition on the magnetic moment is violated and the energy no longer depends only on the magnitude of the magnetic field. The top becomes unstable in the radial direction.

The drive system shown in Fig. 4 couples to a residual transverse magnetization in the small ring magnet that is part of the top. Other drive variations also work including straight

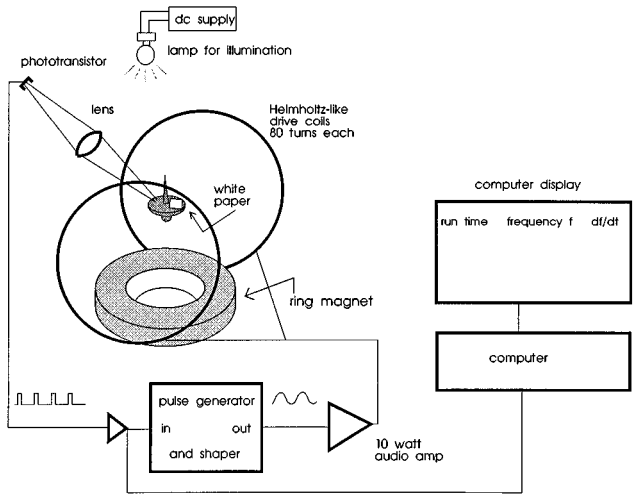

Fig. 4. Experimental setup for synchronous drive of the top to overcome slowing due to air resistance or to increase the spin rate. By slowly increasing the spin, the upper spin limit can be observed.

wires laid across the base magnet and a rotating field made with coils driven 90° out of phase at around 20 Hz. If the temperature does not fluctuate too much, the driven systems can levitate indefinitely.

The lower spin limit for the top corresponds to the condition for a ''sleeping'' top. A sleeping top is a fast top, that when started vertically, remains vertical. The minimum speed ω required for a sleeping top is given by the relation

$$\frac{\omega}{\omega_p} \geqslant 4\,\frac{I_t}{I}$$

or

$$\omega \geqslant \frac{2}{r_{\text{eff}}}\,\sqrt{\frac{\mu}{m}\,B\,\frac{I_t}{I}}\,, \tag{11}$$

where r_{eff} is the effective radius for the moment of inertia $I=mr_{\text{eff}}^2$ of the top and I_t is the moment of inertia around an axis transverse to the main spin axis. For practical tops the ratio of the moments of inertia is between 1 and 1/2. At the low frequency limit the top tips over enough that the magnetic field gradient can no longer support it and it falls.

A condition for the possibility of stable levitation is that the upper spin limit must be higher than the lower spin limit. While this sounds trivial, there is no guarantee that for realizable systems the maximum frequency is not below the minimum. From Appendix A Eq. (17) and Eq. (11) we can get an expression for the ratio of the maximum to minimum spin frequency,

$$\frac{\omega_{\max}}{\omega_{\min}}=\frac{B_0\mu}{2r_{\text{eff}}\,mg}\,\sqrt{\frac{I}{I_t}}\,. \tag{12}$$

For tops that are nearly all magnetic material, the ratio μ/m is essentially a material property, the magnetic moment per unit mass. For the materials and configuration used with some of our homemade tops the permissible spins were measured to be in the range of 1000–3000 rpm, and the undriven float time as much as 4 min in air. Attempts to achieve longer levitation by spinning the top faster run into trouble with the upper spin limit.

Measurements on top parameters were made and compared with the analytical theory and a computer simulation of the top motion. The computer simulation does not make the fast top approximation that all the angular momentum is along the top axis and follows the full rotational dynamics. The equations used in the simulation are described in Appendix B. The simulation monitors the top center of mass in x, y, and z, the projection of the top spin axis on the x-y plane, and $\mu_{\|}=\boldsymbol{\mu}\cdot\mathbf{B}/B$ as the spin frequency is slowly ramped. One can clearly see the top start to go unstable when the component of $\boldsymbol{\mu}$ along $\mathbf{B}$ begins to change near the upper spin frequency limit. The simulation can investigate both the upper and lower stability bound.

We describe here how some of the top parameters were measured for the commercial Levitron top and an experimental stemless top on both the Levitron base magnet as well as an adjustable experimental circular base magnet. The stemless top was developed so that its rotational inertia could be more accurately determined by geometry alone. Instead of using weights, adjustment is achieved by changing the spacing between two ring magnets that make up the base. The rotational inertia of the Levitron top, with weights, was determined by a torsion wire method. The earth's field had to

Table I. Measured and computed values for three different top-base configurations.

	Levitron base and top	Exp. base 1, Levitron top	Exp. base 2, stemless top
top mass m	0.021 35 kg	0.021 35 kg	0.0152 kg
mag. mom. μ	0.65 A m^2	0.65 A m^2	0.46 A m^2
μ/m	30.4 A m^2/kg	30.4 A m^2/kg	30.3 A m^2/kg
rot. inert. I	2.20×10^{-6} kg m^2	2.20×10^{-6} kg m^2	1.63×10^{-6} kg m^2
transv. in. I_t	1.32×10^{-6} kg m^2	1.32×10^{-6} kg m^2	0.865×10^{-6} kg m^2
I_t/I	0.60	0.60	0.53
r_{eff}	0.0102 m	0.0102 m	0.0104 m
B_0	0.0136 T	0.0205 T	0.0173 T
S	-0.322 T/m	-0.322 T/m	-0.324 T/m
K	1.12 T/m^2	0.594 T/m^2	1.05 T/m^2
η	0.70	1.12	0.45
$\gamma_{\max}$	0.87	0.84	0.89
Upper frequency limit			
linear theory	227 rad/s	412 rad/s	321 rad/s
simulation	251 rad/s	436 rad/s	327 rad/s
experiment	254 rad/s	332 rad/s	291 rad/s
Lower frequency limit			
sleeping top	98 rad/s	120 rad/s	102 rad/s
simulation	98 rad/s	120 rad/s	103 rad/s
experiment	114 rad/s	129 rad/s	122 rad/s

be cancelled with another magnet and the wire torsional spring constant was calibrated with known spheres. The magnetic moments μ of the tops were determined with a compass needle aligned with the earth's field and a calibrated coil. The top dipole caused a deflection of the compass needle which was nulled out by a current through the coil. From this current the dipole moment could be determined more accurately than from gaussmeter measurements alone. The field gradient S at the levitation point was determined from Eq. (9).

A technique similar to NMR was used to find the precession frequency ω_p and the bounce frequency Ω_z described in Appendix A. First, the top was driven at a constant frequency ω with the system shown in Fig. 4. A small drive coil was arranged to couple to either the precession or the axial bounce motion and then pulsed, to drive the mode. The resulting oscillation was then sensed by the same coil and fed to a narrow band amplifier and frequency counter. ω_p could be measured to about 1% accuracy while Ω_z could only be measured to within 10% due to coupling between the axial and radial oscillations. B_0 and K were then determined from Eqs. (3) and (14). Hall gaussmeter measurements of B_0, S, and K were in reasonable agreement with the above method but are considered less accurate.

Below we present a table of values (see Table I) for three of the cases we measured and compared to the linear theory and the computer simulation. In general, the experimental results agree with the theory and simulation to within 20%. In most cases, the experiment does not reach the calculated upper frequency limit and in all cases, does not quite reach the lower frequency limit. We believe that there could be errors in our value for B_0. While we can measure the precession frequency ω_p very precisely at any spin frequency ω, we found that our calculation of B_0 depended on the spin frequency in a way which we don't fully understand yet. Errors in B_0 affect the calculation of the upper and lower spin limits. It is also worth mentioning here that the top is not really a point dipole, but a large (compared to the potential well) ring magnet. To do a better job, one should integrate over the whole magnet.

The depth of the energy well can be estimated from the observed bounce frequency in the well, about 1 Hz, and the excursion amplitude, about 5 mm. The well depth is on the order of 10^{-5} J. If we were trying to trap a 20-g top in a gravitational well of the same depth we would be trying to catch it in a depression only 50 μm deep. This limits how much translational energy the top can have when trying to insert it into the levitation region.

One mysterious feature of the Levitron has been the need to constantly adjust the weight of the top, even over a period of a few minutes. Our experiments showed that this was due to temperature variation due to handling and ambient temperature changes. The ceramic magnets used have a reversible demagnetization temperature coefficient of about 0.2% per °C. Cooling the magnets increases their field strength and requires the top to be heavier to levitate.

III. MATERIALS TO EXPERIMENT WITH

Base magnets can be ring magnets or an array of barrel, bar, or disk magnets. Usable large (10-cm o.d.) ring magnets can be found on speakers or in microwave oven magnetrons. (It is not easy to remove ring magnets from speakers. Sometimes the glue will release in boiling water but not always.) If broken speakers or magnetrons are not available, four bar magnets arranged in a square with their north poles inward, or barrel magnets arranged in a square or circle with their north poles up can be used. These will have to be put on a steel plate or glued to prevent them from moving. A steel plate will also have the effect of increasing the field strength and allow the magnet positions to be adjusted. Rings with larger mean radius have a higher levitation point but a weaker field and gradient at the levitation point. Small ring magnets for the spinning top can be found at Radio Shack, five for less than $2 but they are weaker than the tops that

come with the Levitron and require a stronger gradient to levitate. The capture volume is quite small and the weight of the top critical so quite a bit of fussing is usually required. The weight must be adjusted to within approximately 0.2 g.

When weighted correctly the top does very little nodding around the well. The top can sometimes be straightened up by raising and lowering the lifter plate a few times below the levitation region. The lifter plate can also be used to damp out some of the vertical oscillation after the top has left the plate. If the base magnet is not uniformly magnetized, it will need to be tilted so that the field at the levitation region is level. Sometimes the magnetic moment of a homemade ring magnet top is not purely axial. A small transverse moment makes the top easier to drive (as in Fig. 4), but it also makes the top fall down sooner.

APPENDIX A: LINEAR PRECESSING MODEL

To derive the upper spin limit for the top and some of the other dynamics, we need to go back to the equations of motion. While our computer solution of the equations of motion keeps terms to second order, the upper spin frequency condition can be derived from the linearized equations. We write Eqs. (1) and (2) in terms of our field expansion. For the z component we have

$$\frac{d^2z}{dt^2}=-2K\,\frac{\mu}{m}\,z-\left[g+\frac{\mu}{m}\,S\right]. \tag{13}$$

The term in the brackets is zero at the levitation point. The top is trapped in z and oscillates at a frequency

$$\Omega_z=\sqrt{\frac{2K\mu}{m}}, \quad z=z_0\,\cos\,\Omega_z t. \tag{14}$$

Defining $\omega_p=-\mu B_0/I\omega$ so that ω_p changes sign when ω changes sign, the other equations are

$$\begin{aligned}
\frac{d\mu_x}{dt}&=-\omega_p\mu_y-\frac{S\mu^2}{2I\omega}\,y,\\
\frac{d\mu_y}{dt}&=+\omega_p\mu_x+\frac{S\mu^2}{2I\omega}\,x,\\
\frac{d^2x}{dt^2}&=-\frac{S}{2m}\,\mu_x+\frac{\mu K}{m}\,x,\\
\frac{d^2y}{dt^2}&=-\frac{S}{2m}\,\mu_y+\frac{\mu K}{m}\,y.
\end{aligned} \tag{15}$$

We change to complex variables $\mu_\perp=\mu_x+i\mu_y$ and $u=x+iy$ and solve by substituting $\mu_\perp=\mu_0 e^{i\alpha t}$ and $u=u_0e^{i\alpha t}$. The result is a cubic equation for α. The condition that the motion be bounded is that all three roots of the cubic are real. From this the condition for stability can be derived and is $\gamma<\gamma_{\max}$, where

$$\begin{aligned}
\gamma&=\omega r_{\rm eff}^2\,g\left(\frac{m}{\mu B_0}\right)^{3/2},\\
\gamma_{\max}&=\sqrt{\frac{1+\eta}{2}\,\{f(\eta)+\sqrt{[f(\eta)]^2+64\eta}\}},\\
f(\eta)&=1-18\eta-27\eta^2,\\
\eta&=\frac{(S/2)^2}{B_0K}-1.
\end{aligned} \tag{16}$$

The function $\gamma_{\max}$ is nearly constant and ranges between 0.77 and 1. It is approximated by the simpler function

$$\gamma_{\max}\approx\frac{1+\dfrac{4}{3\sqrt{3}}\,2\eta}{1+2\eta}$$

within 0.36%. These relations determine the upper spin limit for stable operation. The absolute upper spin limit, setting $\eta=0$, is

$$\omega\leqslant\frac{1}{r_{\rm eff}^2\,g}\left(\frac{\mu B_0}{m}\right)^{3/2}. \tag{17}$$

The analytical results have been confirmed by computer simulation of the complete equations (see Appendix B) and by experiment within 20%.

APPENDIX B: ANALYTIC MODEL WITHOUT THE ''FAST'' TOP ASSUMPTION

At the cost of some complication a model without the fast top assumption may be constructed.

Joos[12] considers a symmetrical top that has been set into rotation about its figure axis, which is designated as the $\mathbf{k}'$ axis. After the initial spinup no moments are applied about the figure axis ensuring that $\omega_{z'}$ is constant. He then writes the angular velocity vector as the sum of a component along the figure axis of the top $\boldsymbol{\omega}_{z'}$, and a component $\boldsymbol{\Omega}_{n'}$ normal to the figure axis:

$$\boldsymbol{\omega}=\boldsymbol{\Omega}_{n'}+\boldsymbol{\omega}_{z'}.$$

The angular momentum vector

$$\mathbf{L}=I_t\boldsymbol{\Omega}_{n'}+I\omega_{z'}\mathbf{k}'.$$

I_t is the moment of inertia about an axis perpendicular to the figure axis. Differentiating,

$$\frac{d\mathbf{L}}{dt}=\mathbf{M}=I_t\,\frac{d\boldsymbol{\Omega}_{n'}}{dt}+I\omega_{z'}\,\frac{d\mathbf{k}'}{dt}. \tag{18}$$

Noting that

$$\frac{d\mathbf{k}'}{dt}=\boldsymbol{\Omega}_{n'}\times\mathbf{k}', \tag{19}$$

we also have $\mathbf{M}=I_t(d\boldsymbol{\Omega}_{n'}/dt)+I\omega_{z'}\boldsymbol{\Omega}_{n'}\times\mathbf{k}'$. Solving for the derivative of $\boldsymbol{\Omega}_{n'}$,

$$\frac{d\boldsymbol{\Omega}_{n'}}{dt}=\frac{\mathbf{M}-I\omega_{z'}\boldsymbol{\Omega}_{n'}\times\mathbf{k}'}{I_t}. \tag{20}$$

With the derivatives of $\boldsymbol{\Omega}_{n'}$ and $\mathbf{k}'$ in hand [Eqs. (19) and (20)], one may now integrate forward the motion of the top by standard differential equation solvers. This has been done with the torque $\mathbf{M}=\boldsymbol{\mu}\times\mathbf{B}$, $\boldsymbol{\mu}$ in the $-\mathbf{k}'$ direction, and the motion of the center of mass determined by Eq. (2), and the model successfully predicts the observed high- and the low-frequency spin speed stability limits to within 20%. It also illustrates the mechanism of loss. At the low-frequency limit the top tips over enough so the magnetic field gradient no longer supports it. At the high-frequency limit the trapping in the horizontal plane gets softer and softer, and the top eventually wanders away.

[a)]Electronic mail: msimon@physics.ucla.edu

[1]Distributed by Fascinations, Seattle, WA.
[2]D. Kagan, ''Building a magnetic levitation toy,'' Phys. Teach. **31**, 432–433 (1993).
[3]S. Earnshaw, ''On the nature of the molecular forces which regulate the constitution of the luminiferous ether,'' Trans. Cambridge Philos. Soc. **7**, 97–112 (1842).
[4]U.S. Patent 5,404,062 E. W. and W. G. Hones (1995).
[5]R. Edge, ''Levitation using only permanent magnets,'' Phys. Teach. **33**, 252–253 (1995) and ''Corrections to the levitation paper,'' *ibid.* **34**, 329 (1996).
[6]U.S. patent 4,382,245 R. M. Harrigan (1983).
[7]R. Harrigan (private communication).
[8]B. Hones (private communication); written communication from his patent attorney.
[9]M. V. Berry, ''The Levitron™: An adiabatic trap for spins,'' Proc. R. Soc. London, Ser. A **452**, 1207–1220 (1996).
[10]V. V. Vladimirskii, ''Magnetic mirrors, channels and bottles for cold neutrons,'' Sov. Phys. JETP **12**, 740–746 (1961); W. Paul, ''Electromagnetic traps for charged and neutral particles,'' Rev. Mod. Phys. **62**, 531–540 (1990).
[11]A. L. Migdall, J. V. Prodan, W. D. Phillips, T. H. Bergeman, and H. J. Metcalf, ''First observation of magnetically trapped neutral atoms,'' Phys. Rev. Lett. **54**, 2596–2599 (1985).
[12]G. Joos and I. Freeman, *Theoretical Physics* (Hafner, New York, 1950), 2nd ed., pp. 150–156.